

## First-Principles Study of the Magnetic Structure of $\text{Na}_2\text{IrO}_3$

Kaige Hu (胡凯歌), Fa Wang,\* and Ji Feng (冯济)†

*International Center for Quantum Materials, School of Physics,  
Peking University, Beijing 100871, China*

*and Collaborative Innovation Center of Quantum Matter, Beijing 100871, China*

(Received 8 April 2015; revised manuscript received 12 June 2015; published 16 October 2015)

The iridate  $\text{Na}_2\text{IrO}_3$  was proposed to be a realization of the Kitaev model with a quantum spin liquid ground state. Experiments have now established that this material hosts a zigzag antiferromagnetic order. However, the previous assignment of the ordered moment direction to the  $\mathbf{a}$  axis is controversial. We examine the magnetic moment direction of  $\text{Na}_2\text{IrO}_3$  using the local spin density approximation plus spin orbit coupling+U calculations. Our calculations reveal that the total energy is minimized when the zigzag-ordered moments are aligned along  $\mathbf{g} \approx \mathbf{a} + \mathbf{c}$  direction. The dependence of the total energy on moment directions can be explained by adding anisotropic interactions to the nearest-neighbor Kitaev-Heisenberg model, on which the spin-wave spectrum is also calculated. The revision of ordered moments is very important to understanding and achieving possible exotic electronic phases in this compound.

DOI: 10.1103/PhysRevLett.115.167204

PACS numbers: 75.10.Jm, 75.10.Kt, 75.25.-j, 75.30.Et

Iridium-based  $5d$  transition metal oxides display rich and interesting properties owing to the interplay of spin-orbit coupling (SOC), electron correlation, and crystal-field splitting [1–6]. In particular,  $A_2\text{IrO}_3$  ( $A = \text{Na}, \text{Li}$ ) have attracted special attention [5–16]. The structures of these materials contain layered honeycomb lattices of Ir atoms. Each  $\text{Ir}^{4+}$  ion is surrounded by an oxygen octahedron and would possess an effective  $j_{\text{eff}} = 1/2$  pseudospin, and the edge-sharing oxygen octahedron structure was proposed to realize the Kitaev model [5,6]. As an exactly solvable quantum spin-1/2 system, the Kitaev model embodies a quantum spin liquid ground state and Majorana fermionic excitations, which have potential applications to quantum computation [17]. However, later experiments have shown that the magnetic structure of  $\text{Na}_2\text{IrO}_3$  is not a spin liquid but zigzag antiferromagnetic (AFM) long range order [13,14]. Better understanding of this magnetic structure will provide important clues on how to realize the Kitaev spin liquid in this family of materials.

Although zigzag AFM order is well established experimentally, the assignment of the AFM moment direction is not without ambiguity. The zigzag AFM order was first proposed by combining resonant magnetic x-ray scattering measurements and first-principles calculations with the ordered moment assigned to the crystallographic  $\mathbf{a}$  axis [12]. In later experiments that confirmed the zigzag configuration with neutron scattering, this assumption of moment direction was inherited without further scrutiny [13,14]. This moment direction assignment is inconsistent with first-principles calculations: previous calculations predicted that the zigzag configuration has lower total energy for magnetic moments along the  $\mathbf{b}$  axis compared to the  $\mathbf{a}$  axis [12].

The determination of the ordered moment direction is critical for establishing a reliable microscopic model of the

low energy physics in this compound. Various modifications to the Kitaev model, in particular the Kitaev-Heisenberg (KH) model, have been suggested to accommodate the zigzag order [7,9,11,13,18]. However, the anisotropic Kitaev interaction favors the moment direction along the  $\hat{z}$  axis of the local  $\text{IrO}_6$  octahedron. Several recent studies [19–24] analyzed the necessity of adding other anisotropic interactions to the KH Hamiltonian, which was expected to stabilize the zigzag configuration. But a complete and falsifiable explanation for the moment direction puzzle remains evasive.

In this Letter, we examine the energetics of  $\text{Na}_2\text{IrO}_3$ , sampling a wide range of magnetic order with different moment alignments using the local spin density approximation plus SOC and effective Hubbard  $U$  (LSDA + SOC + U) calculations. Our calculations show that the ground state is attained in the zigzag AFM structure, with a moment direction  $\mathbf{g} \approx \mathbf{a} + \mathbf{c}$ . We further show that the energy dependence on moment directions can be well fitted with a modified nearest-neighbor Kitaev-Heisenberg (nnKH) Hamiltonian by adding anisotropic interactions, in which the Kitaev term still dominates. Based on this model, we derive a few experimentally accessible quantities, such as the spin wave spectrum. Finally, we clarify that this assignment of moment direction is also consistent with the resonant x-ray magnetic scattering measurements [12].

$\text{Na}_2\text{IrO}_3$  is a layered compound (space group  $C2/m$ ), in which Ir ions are located at the centers of edge-sharing oxygen octahedra [Fig. 1(a)] [13,14], and form honeycomb lattices within each layer. Each  $\text{Ir}^{4+}$  ion has five  $5d$  electrons, occupying  $t_{2g}$  orbitals of the ideal octahedral crystal field, assuming the oxygen octahedra remain regular. Owing to the strong spin-orbit coupling, the six  $t_{2g}$  spin orbitals are further separated into two manifolds with, respectively,  $j_{\text{eff}} = 3/2$  and  $j_{\text{eff}} = 1/2$  [5]. The bands

mainly composed of the  $j_{\text{eff}} = 3/2$  states are fully filled, while the spin-orbit-coupled  $j_{\text{eff}} = 1/2$  states are half filled. Khaliulin *et al.* [6] first analyzed this electronic structure and suggested that this material can be described by the Kitaev's spin-1/2 model with a spin liquid ground state. Later experiments, however, discovered zigzag AFM order in this material [13,14]. Several theoretical models have since been proposed to account for the magnetic order in  $\text{Na}_2\text{IrO}_3$ , including (i) the nnKH model, which only includes nearest-neighbor interaction between Ir atoms [6,7], (ii) the KH- $J_2 - J_3$  model which also includes the second and third nearest neighbor Heisenberg hopping  $J_2$  and  $J_3$  between Ir atoms [9,11,13,18], (iii) the *modified* nnKH model which includes additional anisotropic interactions besides Kitaev terms and Heisenberg terms [19–23], and (iv) the quasimolecular orbital model [25–27]. Four types of magnetic orders, ferromagnetic (FM), Néel AFM, stripy AFM, and zigzag AFM, as shown in Fig. 1(b), can be realized in these models depending on model parameters.

The nnKH model is the simplest model that can produce the zigzag AFM ground state, with the following Hamiltonian [7]:

$$H = \sum_{\gamma=x,y,z} \sum_{\langle ij \rangle \in \gamma} (2KS_i^\gamma S_j^\gamma + JS_i \cdot S_j), \quad (1)$$

where the first term is the strongly anisotropic Kitaev interaction [17] [ $\gamma = x, y, z$  refers to the three nn bonds and

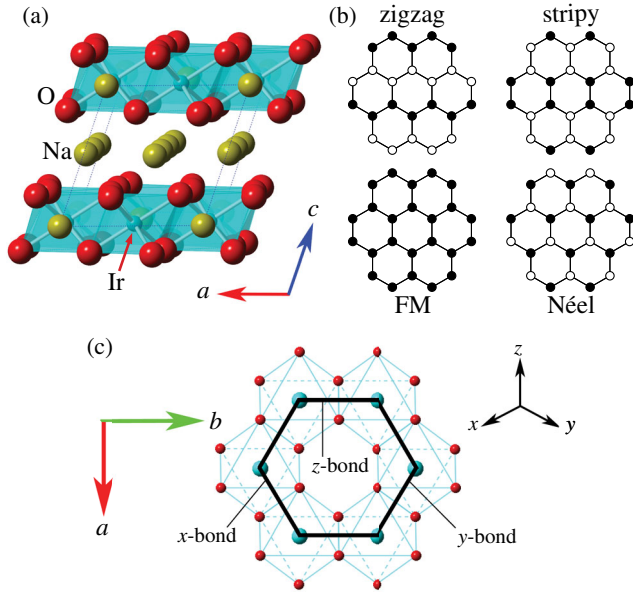


FIG. 1 (color online). (a) The  $C2/m$  crystal structure of  $\text{Na}_2\text{IrO}_3$ , viewed from slightly off the  $b$  direction. (b) Four different types of magnetic order. White and black circles denote up and down spins, respectively. (c) Three different types of nearest-neighbor Ir-Ir bonds. The iridium honeycomb planes are perpendicular to the cubic direction [111].

also the three local axes along the Ir-O bonds of the  $\text{IrO}_6$  octahedron shown in Fig. 1(c)], and the second term describes the Heisenberg interaction. Equation (1) can be rewritten as Ref. [7]  $H = \sum_{\gamma} \sum_{\langle ij \rangle \in \gamma} A(2 \sin \zeta S_i^\gamma S_j^\gamma + \cos \zeta \mathbf{S}_i \cdot \mathbf{S}_j)$ , where  $A = \sqrt{K^2 + J^2}$  is a positive energy scale and the “phase” angle  $\zeta$  tunes the sign and relative strength of the Kitaev and the Heisenberg interactions. The anisotropic energy for the four possible magnetic patterns, i.e., FM, Néel, stripy, and zigzag, can be expressed as  $E_{\text{zigzag}} = (A/2)[\cos \zeta - 2 \sin \zeta \cos(2\theta)]$ ,  $E_{\text{stripy}} = -E_{\text{zigzag}}$ ,  $E_{\text{FM}} = (A/2)(3 \cos \zeta + 2 \sin \zeta)$ , and  $E_{\text{Néel}} = -E_{\text{FM}}$ , where  $\theta$  is the polar angle of the magnetic moment in the local spherical coordinates of the  $\text{IrO}_6$  octahedron. Figure 2(a) shows that when the zigzag magnetic order is the ground state ( $\zeta = 3\pi/4$  in the figure), the magnetic moments point along the local  $\hat{z}$  direction. This conclusion is consistent with the assumptions in a neutron experiment reported in Ref. [13]. The KH- $J_2 - J_3$  model should produce the same results on the anisotropic energy since the Heisenberg terms are isotropic.

Motivated by the foregoing analysis, we perform detailed investigations on the anisotropic energy by non-collinear relativistic density functional theory with full self-consistent fields, as implemented in the Vienna *ab initio* simulation package [28,29]. The experimental lattice structure of  $\text{Na}_2\text{IrO}_3$  is adopted [13]. The experimentally determined magnetic unit cell contains two antiferromagnetically coupled layers of Ir atoms [12]. However, the magnetic unit cell in our calculations is chosen to contain only one layer of Ir atoms. It is reasonable since the coupling between Ir honeycomb lattices is negligibly small (see Supplemental Material, Ref. [30]). Such a choice is also consistent with the KH model, which takes no account of the coupling between Ir honeycomb layers. The projector-augmented wave potentials [31] with a plane-wave cutoff of 500 eV is employed. We use the Monkhorst-Pack  $k$ -point meshes [32] of  $6 \times 4 \times 6$  per magnetic unit cell to perform the Brillouin zone summation. We set  $U = 1.7$  and  $J = 0.6$  eV [33], which corresponds to  $U_{\text{eff}} = U - J = 1.1$  eV [34]. This choice of  $U_{\text{eff}}$  results in a band gap of 341 meV for the zigzag-ordered ground state, consistent with the experimentally measured values (340 meV in Ref. [8]). In the Supplemental Material [30] we show that our main conclusion about the moment direction is insensitive to the choice of  $U$ . To survey the potential energy surface of magnetization, the spin magnetic moment is constrained in specified directions while the magnitude is optimized.

Figure 2(b) shows the total energies of the four magnetic configurations with magnetic moments lying in the  $ac$  plane for the experimental structure of  $\text{Na}_2\text{IrO}_3$ . The horizontal axis is the angle between the total moment and the  $a$  axis, where the total moment is the summation of the spin and orbital moments. Surprisingly, although the zigzag state is indeed the ground state, the total moment of the lowest-energy configuration points along *neither* the

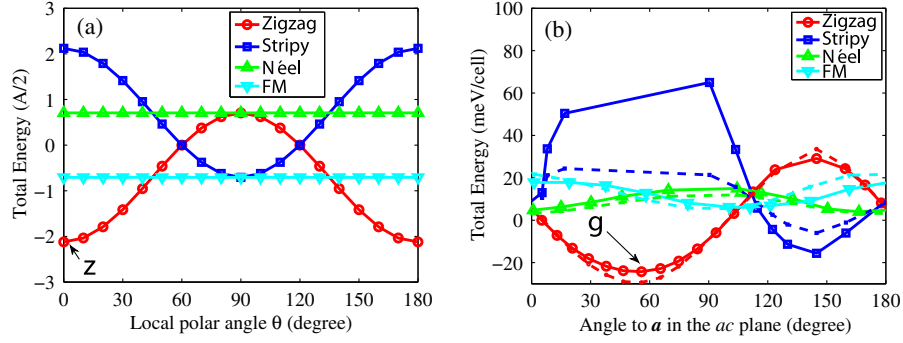


FIG. 2 (color online). (a) Anisotropic energy of the KH model in the  $\zeta = 3\pi/4$  zigzag state. The angle  $\theta$  is the polar angle in the local spherical coordinates of the  $\text{IrO}_6$  octahedron. (b) Anisotropic energy in the  $ac$  plane by LSDA + SOC + U calculations (solid lines) versus the total moment for the experimental structure of  $\text{Na}_2\text{IrO}_3$ . Angles are measured from the  $\mathbf{a}$  axis. The energy of the zigzag order with the moment along the  $\mathbf{a}$  axis is set to be 0. Corresponding fitted curves are also shown (dashed lines).

cubic  $\hat{z}$  axis suggested by the KH model, *nor* the crystallographic  $\mathbf{a}$  axis suggested in Ref. [12]. When the moment sweeps the  $ac$  plane, the total energy is minimized along the direction  $\mathbf{g} \approx \mathbf{a} + \mathbf{c}$ , which forms an angle of roughly  $55^\circ$  with the  $\mathbf{a}$  axis [see Fig. 3(a)]. The  $\mathbf{g}$  configuration's energy is significantly lower than the  $\mathbf{a}$  configuration by about 24 meV per unit cell (4 Ir). As shown in Fig. 3(b),  $\hat{\mathbf{g}}$  is the intersection between a unit circle spanned by  $\hat{\mathbf{a}} - \hat{\mathbf{c}}$  and one by local  $\hat{\mathbf{x}} - \hat{\mathbf{y}}$ . It is interesting to note that  $\mathbf{g}$  is a high-symmetry direction of the local  $\text{IrO}_6$  octahedron, [110], pointing toward the center of one of the O-O edges. The anisotropic energy reaches its maximum value in the  $ac$  plane when the total moment points to the cubic  $\hat{z}$  axis.

Figure 4 further confirms that the  $\mathbf{g}$  direction is actually the moment direction of the zigzag ground state. The anisotropic energy is computed with the spin moment moving in three different planes: the  $ac$ ,  $ab$ , and  $gb$  planes [see Fig. 3(b)]. The scanned moment angles are measured from the  $\mathbf{a}$  direction for the  $ac$  and  $ab$  plane, and from the  $\mathbf{g}$  direction for the  $gb$  plane, respectively. The horizontal axes are the angle of the spin moment in Fig. 4(a) and the angle of the total moment in Fig. 4(b), respectively. The spin and orbital moments are nearly collinear, with mutual angles less than  $15^\circ$ . As a consequence, the curves in Fig. 4(a) are similar to that in Fig. 4(b). For the zigzag configuration, the angle of the  $\mathbf{g}$  direction relative to the  $\mathbf{a}$  axis is about  $60^\circ$  for the spin moment and roughly  $55^\circ$  for the total moment. The total moment is ideally located in the cubic  $xy$  plane of the  $\text{IrO}_6$  octahedron. When the moment points along the  $\mathbf{a}$  axis, the energy is higher than that of both the  $\mathbf{b}$  and  $\mathbf{g}$  directions. The energy with the moment pointing along the  $\mathbf{b}$  axis is a saddle point on the potential energy surface: it is the minimum in the  $ab$  plane and the maximum in the  $gb$  plane (i.e., the cubic  $xy$  plane). It is higher than the ground energy (that of the  $\mathbf{g}$  direction) by 9.4 meV per unit cell. We conclude that the  $gb$  plane (the cubic  $xy$  plane) is an “easy” plane. Moreover, the  $\mathbf{g}$  configuration of ground magnetic structure is consistent with resonant x-ray magnetic scattering measurement, which suggests that magnetic moments lie in the  $ac$  plane [12,15].

Now we turn to the model explanation of the computed magnetic anisotropy. The prediction of magnetic moments along the  $\hat{z}$  axis indicates that the KH model is clearly inadequate. Here, we show that the  $\mathbf{g}$  direction assignment of magnetic moment can be explained by a modified nnKH model with additional anisotropic interactions, in which the parameters can be fitted from the LSDA + SOC + U energies. The generalized model is described as

$$H = \sum_{\alpha,\beta=x,y,z} \sum_{\langle ij \rangle} S_i^\alpha J_{ij}^{\alpha\beta} S_j^\beta, \quad (2)$$

where the  $3 \times 3$  matrices  $J_{ij}$  on the  $x$ ,  $y$ ,  $z$  bonds are

$$\begin{pmatrix} J + 2K & J_{\parallel\perp} & J_{\parallel\perp} \\ J_{\parallel\perp} & J & J_{\perp\perp} \\ J_{\parallel\perp} & J_{\perp\perp} & J \end{pmatrix}, \quad \begin{pmatrix} J & J_{\parallel\perp} & J_{\perp\perp} \\ J_{\parallel\perp} & J + 2K & J_{\parallel\perp} \\ J_{\perp\perp} & J_{\parallel\perp} & J \end{pmatrix}, \\ \begin{pmatrix} J & J_{\perp\perp} & J_{\parallel\perp} \\ J_{\perp\perp} & J & J_{\parallel\perp} \\ J_{\parallel\perp} & J_{\parallel\perp} & J + 2K \end{pmatrix},$$

respectively.

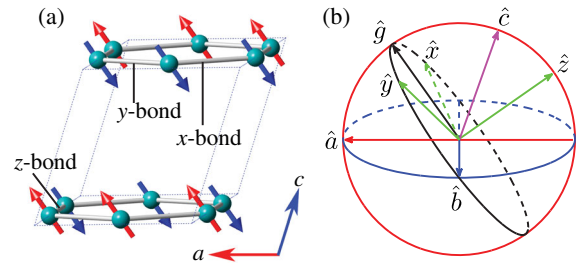


FIG. 3 (color online). (a) The Ir honeycomb structure of  $\text{Na}_2\text{IrO}_3$  and the zigzag magnetic order of the magnetic ground state. (b) Relative relations of the local  $\text{IrO}_6$  axes  $\hat{\mathbf{x}}$ ,  $\hat{\mathbf{y}}$ , and  $\hat{\mathbf{z}}$ , the crystallographic axes  $\mathbf{a}$ ,  $\mathbf{b}$ , and  $\mathbf{c}$ , and also the moment direction  $\mathbf{g}$ .

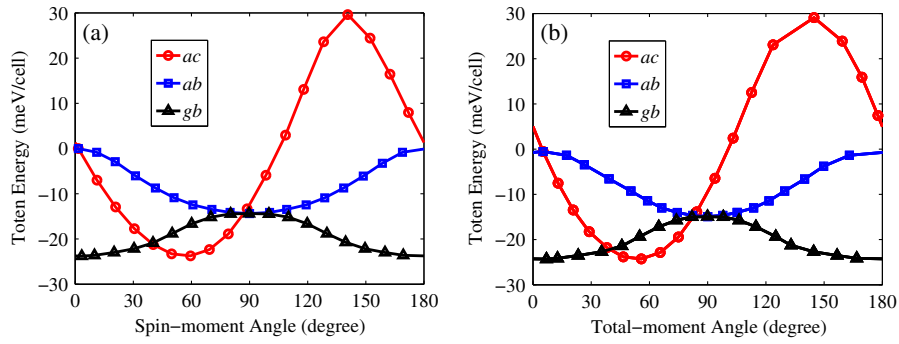


FIG. 4 (color online). (a) Anisotropic energy by LSDA + SOC + U calculations for the spin moments in three different planes:  $ac$ ,  $ab$ , and  $gb$ . Angles are measured from the  $a$  axis to the moment direction for the  $ac$  and  $ab$  plane, and from the  $g$  direction for the  $gb$  plane, respectively. (b) Corresponding anisotropic energy by LSDA + SOC + U calculations versus the total moment direction (solid lines). Corresponding fitted curves by the modified nnKH model are also shown (dashed lines).

The form of these anisotropic exchange interactions is fixed by the assumption of perfect honeycomb lattice symmetry ( $D_{3d}$  symmetry at Ir sites), and has been reported before [22]. The lower symmetry of real  $\text{Na}_2\text{IrO}_3$  crystals will, in principle, produce more complex anisotropies [19], which we will, however, not consider in this work. In fitting the energies we treat the (pseudo-)spins  $S_i^a$  as classical vectors. This model can naturally explain the zigzag AFM ground state without invoking more extended interactions. It can also produce the local [110] moment direction for the zigzag state. The fitted curves are plotted in Fig. 4(b) (dashed lines), with model parameters from the second column of Table S1 in the Supplemental Material [30], where details of the fitting results are also presented. The fitting turns out to be quite good.

From the energy dependence of moment direction for the zigzag AFM state shown in Fig. 4(b), we can fit the Kitaev term coefficient  $K$ , and anisotropy terms  $J_{\parallel\perp}$  and  $J_{\perp\perp}$ . The energies of other magnetic orders shown in Fig. 2(b) are required to fit the Heisenberg couplings. Note that although the modified nnKH model can explain the  $g$ -direction moment assignment of the zigzag state, more interactions are necessary to satisfy the condition for a zigzag ground state. The fitted curves are plotted in Fig. 2(b) (dashed lines), with model parameters from the second column of Table S3 in the Supplemental Material [30], where details of the fitting results are also presented. Within this model, it is uncovered that the dominant interaction is a ferromagnetic Kitaev term.

From the fitted model parameters one can compute several experimentally relevant properties. Figure 5 shows the calculated spin-wave spectrum. It has a significant spin gap (about  $20.8 \text{ meV} \times S = 10.4 \text{ meV}$ ) for spin-wave excitations, which can, in principle, be measured by future inelastic neutron scattering experiments. We note that a resonant inelastic x-ray scattering experiment [35] reported dispersive magnetic excitations with lowest energy of 10 and highest energy of 40 meV, in broad agreement with our calculation. However, we will not make quantitative comparison to this experiment here.

In conclusion, we have proposed an alternative moment direction assignment of the zigzag magnetic order in  $\text{Na}_2\text{IrO}_3$  by a LSDA + SOC + U study. Our results show that the magnetic moments are along the direction  $g \approx a + c$ , forming an angle of roughly  $55^\circ$  with the  $a$  axis, are located in the cubic  $xy$  plane of the  $\text{IrO}_6$  octahedron, and are pointing to the center of the O-O edge. The  $g$  configuration is explained by a modified nnKH model, where additional anisotropic interactions are included.

We would like to emphasize that our proposal (that magnetic moment in  $\text{NaIrO}_3$  lies along the  $g$  direction) is also consistent with all known experimental evidence about moment directions. The most relevant experimental signature to the moment direction is the resonant x-ray magnetic scattering measurements [12], in which the original analysis on the experimental data resulted in an ordered moment along the  $a$  axis. The same experimental data in Ref. [12] have been reanalyzed in Ref. [15],

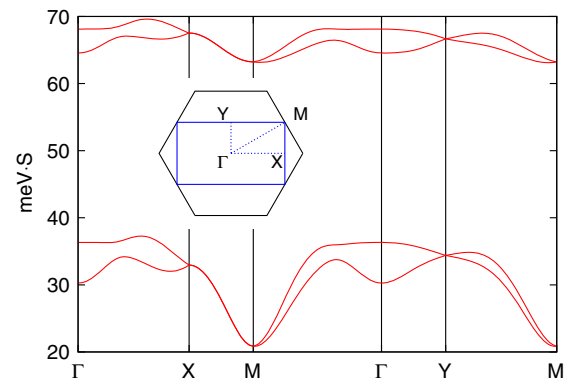


FIG. 5 (color online). Spin-wave spectrum along high symmetry directions for the modified  $\text{KH-}J_2 - J_3$  model under zigzag magnetic order, with parameters in the second column of Table S3 of Ref. [30]. The unit of the vertical axis (energy) is  $\text{meV} \times S$ , where for ideal  $j_{\text{eff}} = 1/2$  state  $S = 1/2$ . Inset depicts the Brillouin zone of the Ir honeycomb lattice. High symmetry points are  $\Gamma(0, 0, 0)$ ,  $X(\pi, 0, 0)$ ,  $M(\pi, \pi, 0)$ , and  $Y(0, \pi, 0)$ .

suggesting that the direction of magnetization makes an angle with the  $c$  axis about  $\omega = 118^\circ$  in the  $ac$  plane. Since the angle enclosed by the  $c$  axis and the  $a$  axis is  $\beta = 109^\circ$ , which is very close to  $118^\circ$ , it was further proposed that magnetic moments were almost parallel to the  $a$  axis. It is, however, crucial to realize that the procedure used by these authors to fit the scattering intensity does not distinguish between  $\pm\omega$ . The angle subtended by the  $c$  axis and the direction of  $-\mathbf{g}$  is  $126^\circ$ , which is also very close to  $118^\circ$ . Note that the moment assignment of  $-\mathbf{g}$  is equivalent to  $\mathbf{g}$  since the zigzag configuration is an AFM state. Therefore, we conclude that the  $\mathbf{g}$  direction is indeed an alternative explanation of the experimental data.

The authors acknowledge support from National Natural Science Foundation of China (Grants No. 11174009 and No. 11374018) and National Basic Research Program of China (973 Program) (Grants No. 2013CB921900, 2011CBA00109, and No. 2014CB920902).

*Note added.*—We are grateful to one of the referees who pointed out that our theoretical assignment of the magnetization direction of  $\text{Na}_2\text{IrO}_3$  was confirmed by a very recent experiment [36].

---

\* wangfa@pku.edu.cn

† jfeng11@pku.edu.cn

- [1] B. J. Kim, H. Jin, S. J. Moon, J.-Y. Kim, B.-G. Park, C. S. Leem, J. Yu, T. W. Noh, C. Kim, S.-J. Oh, J.-H. Park, V. Durairaj, G. Cao, and E. Rotenberg, *Phys. Rev. Lett.* **101**, 076402 (2008).
- [2] B. J. Kim, H. Ohsumi, T. Komesu, S. Sakai, T. Morita, H. Takagi, and T. Arima, *Science* **323**, 1329 (2009).
- [3] X. Wan, A. M. Turner, A. Vishwanath, and S. Y. Savrasov, *Phys. Rev. B* **83**, 205101 (2011).
- [4] D. Pesin and L. Balents, *Nat. Phys.* **6**, 376 (2010).
- [5] G. Jackeli and G. Khaliullin, *Phys. Rev. Lett.* **102**, 017205 (2009).
- [6] J. Chaloupka, G. Jackeli, and G. Khaliullin, *Phys. Rev. Lett.* **105**, 027204 (2010).
- [7] J. Chaloupka, G. Jackeli, and G. Khaliullin, *Phys. Rev. Lett.* **110**, 097204 (2013).
- [8] R. Comin, G. Levy, B. Ludbrook, Z.-H. Zhu, C. N. Veenstra, J. A. Rosen, Y. Singh, P. Gegenwart, D. Stricker, J. N. Hancock, D. van der Marel, I. S. Elfimov, and A. Damascelli, *Phys. Rev. Lett.* **109**, 266406 (2012).
- [9] I. Kimchi and Y.-Z. You, *Phys. Rev. B* **84**, 180407(R) (2011).
- [10] Y. Singh and P. Gegenwart, *Phys. Rev. B* **82**, 064412 (2010).
- [11] Y. Singh, S. Manni, J. Reuther, T. Berlijn, R. Thomale, W. Ku, S. Trebst, and P. Gegenwart, *Phys. Rev. Lett.* **108**, 127203 (2012).
- [12] X. Liu, T. Berlijn, W.-G. Yin, W. Ku, A. Tsvelik, Y.-J. Kim, H. Gretarsson, Y. Singh, P. Gegenwart, and J. P. Hill, *Phys. Rev. B* **83**, 220403(R) (2011).
- [13] S. K. Choi, R. Coldea, A. N. Kolmogorov, T. Lancaster, I. I. Mazin, S. J. Blundell, P. G. Radaelli, Y. Singh, P. Gegenwart, K. R. Choi, S.-W. Cheong, P. J. Baker, C. Stock, and J. Taylor, *Phys. Rev. Lett.* **108**, 127204 (2012).
- [14] F. Ye, S. Chi, H. Cao, B. C. Chakoumakos, J. A. Fernandez-Baca, R. Custelcean, T. F. Qi, O. B. Korneta, and G. Cao, *Phys. Rev. B* **85**, 180403(R) (2012).
- [15] S. W. Lovesey and A. N. Dobrynin, *J. Phys. Condens. Matter* **24**, 382201 (2012).
- [16] H.-J. Kim, J.-H. Lee, and J.-H. Cho, *Sci. Rep.* **4**, 5253 (2014).
- [17] A. Kitaev, *Ann. Phys. (Amsterdam)* **321**, 2 (2006).
- [18] C. H. Kim, H. S. Kim, H. Jeong, H. Jin, and J. Yu, *Phys. Rev. Lett.* **108**, 106401 (2012).
- [19] Y. Yamaji, Y. Nomura, M. Kurita, R. Arita, and M. Imada, *Phys. Rev. Lett.* **113**, 107201 (2014).
- [20] V. M. Katukuri, S. Nishimoto, V. Yushankhai, A. Stoyanova, H. Kandpal, S. Choi, R. Coldea, I. Rousochatzakis, L. Hozoi, and J. van den Brink, *New J. Phys.* **16**, 013056 (2014).
- [21] J. G. Rau, E. K.-H. Lee, and H.-Y. Kee, *Phys. Rev. Lett.* **112**, 077204 (2014).
- [22] J. G. Rau and H.-Y. Kee, [arXiv:1408.4811](https://arxiv.org/abs/1408.4811).
- [23] Y. Sizyuk, C. Price, P. Wölfle, and N. B. Perkins, *Phys. Rev. B* **90**, 155126 (2014).
- [24] J. Chaloupka and G. Khaliullin, *Phys. Rev. B* **92**, 024413 (2015).
- [25] K. Foyevtsova, H. O. Jeschke, I. I. Mazin, D. I. Khomskii, and R. Valentí, *Phys. Rev. B* **88**, 035107 (2013).
- [26] I. I. Mazin, H. O. Jeschke, K. Foyevtsova, R. Valentí, and D. I. Khomskii, *Phys. Rev. Lett.* **109**, 197201 (2012).
- [27] I. I. Mazin, S. Manni, K. Foyevtsova, H. O. Jeschke, P. Gegenwart, and R. Valentí, *Phys. Rev. B* **88**, 035115 (2013).
- [28] G. Kresse and J. Furthmüller, *Phys. Rev. B* **54**, 11169 (1996).
- [29] G. Kresse and J. Hafner, *Phys. Rev. B* **47**, 558 (1993).
- [30] See Supplemental Material at <http://link.aps.org/supplemental/10.1103/PhysRevLett.115.167204> for discussions on (1) the stacking of Iridium honeycomb planes, (2) the propagation direction of the zigzag ordering, (3) the robustness of the moment direction as  $U$  varies, and (4) details of the fitting of the modified KH model parameters.
- [31] G. Kresse and D. Joubert, *Phys. Rev. B* **59**, 1758 (1999).
- [32] H. J. Monkhorst and J. D. Pack, *Phys. Rev. B* **13**, 5188 (1976).
- [33] D. van der Marel and G. A. Sawatzky, *Phys. Rev. B* **37**, 10674 (1988).
- [34] S. L. Dudarev, G. A. Botton, S. Y. Savrasov, C. J. Humphreys, and A. P. Sutton, *Phys. Rev. B* **57**, 1505 (1998).
- [35] H. Gretarsson, J. P. Clancy, Y. Singh, P. Gegenwart, J. P. Hill, J. Kim, M. H. Upton, A. H. Said, D. Casa, T. Gog, and Y.-J. Kim, *Phys. Rev. B* **87**, 220407 (2013).
- [36] S. H. Chun, J.-W. Kim, J. Kim, H. Zheng, C. C. Stoumpos, C. D. Malliakas, J. F. Mitchell, K. Mehlawat, Y. Singh, Y. Choi, T. Gog, A. Al-Zein, M. Moretti Sala, M. Krisch, J. Chaloupka, G. Jackli, G. Khaliullin, and B. J. Kim, *Nat. Phys.* **11**, 462 (2015).